The Role of Correlation in the Operation of Quantum-dot Cellular Automata

Géza Tóth[1] and Craig S. Lent[2]

Abstract - **Quantum-dot Cellular Automata (QCA) may offer a viable alternative of traditional transistor-based technology at the nanoscale. When modeling a QCA circuit, the number of degrees of freedom necessary to describe the quantum mechanical state increases exponentially with the system size. Based on the coherence vector formalism a model is constructed that makes it possible to include only those degrees of freedom that are important from the point of view of the dynamics.**

1 Introduction

In recent years the development of integrated circuits has been essentially based on scaling down, that is, increasing the element density on the wafer. Scaling down of CMOS circuits, however, has its limits. Above a certain element density various physical phenomena, including quantum effects, conspire to make transistor operation difficult if not impossible. If a new technology is to be created for devices of nanometer scale, new design principles are necessary. One promising approach is to move to a transistor-less cellular architecture based on interacting quantum dots, Quantum-dot Cellular Automata (QCA, [1-5]).

A QCA cell consists of four (or five) electrostatically coupled quantum-dots arranged in a square pattern. Information is encoded in the arrangement of charge (i. e., two extra electrons) within the cell. When a cell is switched, these electrons tunnel through interdot barriers to neighboring dots inside the cell.

After developing the basic logic gates the theory has been extended to large arrays of devices and computer architecture questions. A key advance was the realization that by periodically modulating the inter-dot barriers, clocked control of QCA circuitry could be accomplished. The modulation could be done at a rate which is slow compared to inter-dot tunneling times, thereby keeping the switching cells very near the instantaneous ground state. This quasi-adiabatic switching [4] permits both logic and addressable memory to be realized within the QCA framework. It allows a pipe-lining of computational operations.

The ability of modeling large cell arrays is crucial for the development of complex QCA circuits. In a classical electronic circuit the number of state variables (i.e., voltages of capacitors or currents of inductors) increases linearly with the number of building elements. Unfortunately, for a QCA circuit the number of quantum degrees of freedom increases exponentially with the system size. Using the Hartree approximation reduces the number of state variables drastically and it can still give quantitatively good results in many cases. Thus even ignoring many quantum degrees of freedom, the dynamics obtained from the model remains close to the "exact" dynamics obtained from the many-body Schrödinger equation. In other cases, the Hartree method can give quantitatively wrong results.

The intercellular Hartree approximation [3] can reduce the number of state variables since it neglects all intercellular correlations. In general, the correlation of two quantities, A and B can be defined as

$$C_{AB} = \langle AB \rangle - \langle A \rangle \langle B \rangle. \qquad (1)$$

In this paper the role of correlations in the quantum dynamics of QCA circuits is examined. A model is proposed which makes it possible to include as much quantum correlation degrees of freedom as necessary in order to obtain the correct dynamics.

2 Quasi-adiabatic switching with Quantum-dot Cellular Automata

The QCA cell consists of four quantum dots as shown in Fig. 1(a). Tunneling is possible between the neighboring dots as denoted by lines in the picture. Due to Coulombic repulsion the two electrons occupy antipodal sites as shown in Fig. 1(b). These two states correspond to charge polarization +1 and -1, respectively, with intermediate polarizations interpolating between the two.

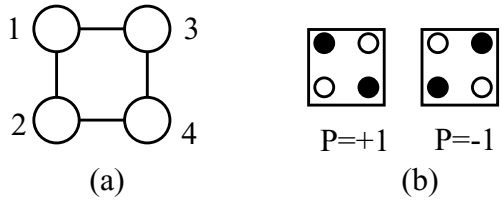

Figure 1: (a) A QCA cell. (b) The two possible charge polarizations.

When placed in proximity, the cells align with each other. A one-dimensional array of cells[4] can be used to transfer the polarization of the driver at one end

[1]Theoretical physics, 1 Keble Rd., OX1 3NP, UK. e-mail: Geza.Toth.17@nd.edu. Home page: http://www.nd.edu/~gtoth. [2]Dept. of Electrical Engineering, University of Notre Dame, IN46556, USA. e-mail: lent@nd.edu.

of the cell line to the other end of the line. Thus the cell line plays the role of the wire in QCA circuits. Moreover, any logical gates (majority gate, AND, OR) can also be implemented, and using these as basic building elements, any logical circuit can be realized[4].

In this paradigm of ground state computing, the solution of the problem has been mapped onto the ground state of the array. However, if the inputs are switched *abruptly*, it is not guaranteed that the QCA array really settles in the ground state, i.e., in the global energy minimum state. It is also possible, that eventually it settles in a *metastable* state because the trajectory followed by the array during the resulting transient is not well controlled.

This problem can be solved by quasi-adiabatic switching [4] of the QCA array. Quasi-adiabatic switching has the following steps: (1) before applying the new input, the height of the interdot barriers is lowered thus the cells have no more two distinct polarization states, P=+1 and P=-1. (2) Then the new input can be given to the array. (3) While raising the barrier height, the QCA array will settle in its new ground state.

The quasi-adiabatic switching is based on the adiabatic theorem, which states that if the change of the Hamiltonian is gradual enough and the system is initially in ground state then it will stay in ground state throughout the whole switching process. Because the system is minimally excited from the ground state, dissipation to the environment is very small.

3 The coherence vector formalism

The Hamiltonian for a QCA circuit modeled as coupled two-state systems [3] is:

$$\hat{H} = -\gamma \sum_{i=1}^{N} \hat{\sigma}_x(i) - \sum_{i=1}^{N-1} \sum_{j=i+1}^{N} \frac{E_{ij}}{2} \hat{\sigma}_z(i)\hat{\sigma}_z(j) + \frac{E_0}{2} \sum_{i=1}^{N} \hat{\sigma}_z(i) P_{driver}(i), \quad (2)$$

where E_{ij} is the electrostatic coupling between cells i and j, and γ is the tunneling energy. The first term describes the intracell tunneling between the two basis states. The second term describes the electrostatic coupling between neighbors. The third term describes coupling to driver cells. For those cells which do not have a driver cell as a neighbor $P_{driver(i)}$=0.

The charge polarization of the k^{th} cell can be interpreted as the expectation value of the $\hat{\sigma}_z(k)$ Pauli spin matrix: $P(k) = -\langle \hat{\sigma}_z(k) \rangle$. With the negative sign we follow the convention of Ref. [6] choosing the sign of the Pauli spin matrices.

The dynamics of the cell line can be computed by the Liouville equation giving the time dependence of the density matrix. The density matrix can be expressed as a linear combination of the s generating operators of the SU(2^N) group:

$$\hat{\rho} = \frac{1}{2^N} \hat{1} + \frac{1}{2^N} \sum_{i=1}^{s} \Lambda_i \hat{\Lambda}_i . \quad (3)$$

where

$$\Lambda_i = \langle \hat{\Lambda}_i \rangle; . \quad (4)$$

The $\hat{\Lambda}_i$ basis operators have the form:

$$\hat{\Lambda}_i = \hat{\lambda}_i^{(1)} \otimes \hat{\lambda}_i^{(2)} \otimes \ldots \otimes \hat{\lambda}_i^{(N)} . \quad (5)$$

where a term of the Kronecker product can be one of four single-cell operators:

$$\hat{\lambda}_i^{(k)} = \begin{cases} \hat{1} \\ \hat{\sigma}_x(k) \\ \hat{\sigma}_y(k) \\ \hat{\sigma}_z(k) \end{cases} . \quad (6)$$

Since choosing only $\hat{1}$'s is excluded, there are s=4^N-1 $\hat{\Lambda}_i$'s.

In this paper the vector constructed from the Λ_i coefficients of the (3) linear combination, the $\vec{\Lambda}$ coherence-vector [6], will be used for the state description instead of the density matrix. The coherence vector can be partitioned into $\vec{\lambda}(i)$ single-cell coherence vectors, $\vec{K}(i, j)$ two-point, $\vec{K}(i, j, k)$ three-point etc., correlation vectors. The $\vec{\lambda}(i)$ single cell coherence vectors contain the expectation values of the $\hat{\sigma}_x(i)$, $\hat{\sigma}_y(i)$ and $\hat{\sigma}_z(i)$ single-cell basis operators. The $\vec{K}(i, j)$ two-point correlation vector has nine elements. They are the expectation values of two-cell basis operators:

$$K_{ab}(i, j) = \langle \hat{\sigma}_a(i)\hat{\sigma}_b(j) \rangle; \quad a, b = x, y, z . \quad (7)$$

Similarly, the elements of the three-point correlations are expectation values of three-cell basis operators:

$$K_{abc}(i, j, k) = \langle \hat{\sigma}_a(i)\hat{\sigma}_b(j)\hat{\sigma}_c(k) \rangle; \quad a, b, c = x, y, z . \quad (8)$$

The dynamics of the coherence vector elements can be obtained by first computing the

dynamics of the basis operators in the Heisenberg picture and then taking the expectation values of both sides of the equations. The differential equation system is linear and has the form:

$$\hbar\frac{d}{dt}\vec{\Lambda} = \hat{\Omega}(t)\vec{\Lambda}, \tag{9}$$

where $\hat{\Omega}(t)$ is the time dependent coefficient matrix. Next the structure of the (9) differential equation system will be presented by giving explicit equations for the single cell coherence vector elements and two-point correlations.

The dynamics of a single cell coherence vector can be obtained as

$$\hbar\frac{d}{dt}\vec{\lambda}(i) = \hat{\Omega}_i\vec{\lambda}(i) + \sum_j E_{ij}\left[K_{yz}(i,j)\ -K_{xz}(i,j)\ 0\right]^T, \tag{10}$$

where

$$\hat{\Omega}_i = \begin{bmatrix} 0 & -E_0P_{driver}(i) & 0 \\ E_0P_{driver}(i) & 0 & 2\gamma \\ 0 & -2\gamma & 0 \end{bmatrix}. \tag{11}$$

The dynamics of the correlation vectors can be obtained as[6]:

$$\hbar\frac{d}{dt}\vec{K}(i,j) = (\hat{1}\otimes\hat{\Omega}_j + \hat{\Omega}_i\otimes\hat{1})\vec{K}(i,j) + \vec{C}_{ij}\{\vec{\lambda}(k),\vec{K}(l,m,n)\}, \tag{12}$$

where $\hat{C}_{ij}$ is an expression consisting of coherence vector elements and three-point correlation vector elements.

Dynamical equations similar to (12) can be written for the three-point, four-point, etc. correlation vector elements. (They are not given here.) The complete set of these differential equations describes the dynamics of the multi-cell system equivalently to the dynamics given by the Liouville equation for the density matrix. We will refer to the model containing the whole set of differential equations for the coherence vector and correlation vector elements as the *exact* model in this paper.

Besides the correlation vector there are other quantities characterizing the intercell correlation. The *correlation vector proper* [6] for two cells has nine elements. They are defined as

$$M_{ab}(i,j) = \langle\left[\hat{\sigma}_a(i) - \langle\hat{\sigma}_a(i)\rangle\right]\left[\hat{\sigma}_b(j) - \langle\hat{\sigma}_b(j)\rangle\right]\rangle, \quad a,b = x,y,z. \tag{13}$$

With coherence vector elements (13) can be rewritten as

$$M_{ab}(i,j) = K_{ab}(i,j) - \lambda_a(i)\lambda_b(j); \quad a,b = x,y,z. \tag{14}$$

The elements of the correlation vector proper are all zero if there is no correlation between the cells or they are *uncorrelated*. The third order correlation vector proper can be defined similarly to (14) with lower order correlation vector and coherence vector elements.

4 Model neglecting higher order correlation

The Hartree approximation assumes that the $M_{ab}(i,i+1)$ two-point correlation vector proper elements are zero (see (14)) and approximates the elements of the two-point correlation vectors with coherence vector elements using $K_{ab}(i,i+1) \approx \lambda_a(i)\lambda_b(i+1)$.

The first approximation, that is better than the Hartree method, can be obtained [7] by keeping only the single cell coherence vectors and the two-point nearest neighbor correlations.

In order to do the truncation of the system of equations, a formula must be constructed to approximate the elements of the $\vec{K}(i,i+1,i+2)$ nearest neighbor three-point correlation vector with nearest neighbor two-point correlation vector and single-cell coherence vector elements. This formula (not shown here) can be deduced from the assumption that the $M_{abc}(i,i+1,i+2)$ three-point correlation vector proper elements and the $M_{ac}(i,i+2)$ next-to-nearest neighbor correlation vector elements are zero. Substituting it into the dynamical equations of nearest neighbor two-point correlations the three-point correlations can be eliminated. The method based on this approximation will be called NNPC referring to that besides the coherence vectors it includes only the nearest neighbor pair correlations in the state description of the cell array [7].

The NNPC method is the simplest that is closer to the exact model with the many-body Hamiltonian than the Hartree method. The number of

state variables scales linearly with the system size for both methods.

The procedure can be generalized. Next-to-nearest neighbor pair correlations and higher than second order correlations can be included and it is also possible to build a model which includes higher order correlations only for those regions where it seems to be necessary.

Since the coherence vector formalism is based on the density matrix description, it is able to model mixed states unlike the state vector description. Dissipation and decoherence can be easily included by adding damping terms to the dynamical equations. This is true for our approximation, as well.

5 Simulation examples

Computer simulations were made to compare NNPC with the Hartree approximation and with the exact model. The comparison was done for the case of quasi-adiabatic switching of a QCA cell line and of a majority gate with unequal input legs. We choose units such that $\hbar$ =1 and E_0=1.

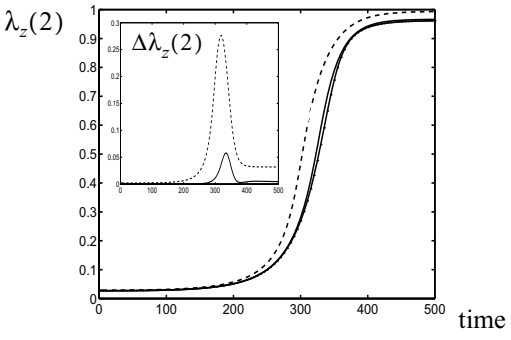

Figure 2. Adiabatic switching of cell line. $\lambda_z(2)$ as the function of time for the Hartree approximation (dashed), NNPC (solid), and the exact model (solid). The inset shows the $\Delta\lambda_z(2)=\lambda_z(2)-\lambda_{z,exact}(2)$ deviation from the exact dynamics for the Hartree method (dashed) and NNPC (solid). NNPC gives a result closer to the exact one than the Hartree approximation does.

The first simulation example is the quasi-adiabatic switching of a line of five cells. The first cell is coupled to a driver cell. The tunneling coefficient is gradually lowered (the barriers are raised). At the end (when the barriers are high) all the cells align with the driver, that is, at the end $\lambda_z(i) = -P(i) \approx 1$. Fig. 2 shows a comparison of the $\lambda_z(2)$ curves corresponding to the Hartree approximation, the NNPC, and the exact model. The inset shows the $\Delta\lambda_z(2)$ deviation from the exact dynamics for the Hartree method (dashed) and NNPC (solid). It is clearly visible that NNPC gives a better match with the exact model than the Hartree approximation does.

The NNPC method also gives the (approximate) dynamics of the nearest neighbor pair correlations thus it is a qualitative improvement compared to the Hartree approximation since the Hartree approximation does not model correlations at all.

The second simulation example is the majority gate with unequal input legs. The Hartree method gives correct results only if the difference in the length of the input legs is smaller than three. By including the correlations of the cross region in the model, it is possible to obtain correct results up to a difference of 39 cells and still use much less degrees of freedom than the exact model.

6 Conclusions

An intermediate model between the Hartree approximation and the exact method was constructed to describe the dynamics of QCA cell arrays. It is based on the truncation of the system of dynamical equations obtained from the coherence vector formalism. By choosing the point of truncation it is possible to include correlation effects to the desired order in the dynamics. The first order differential equation system of real variables obtained this way makes it possible to construct the circuit theoretical model of quantum systems[5].

References

[1] C. S. Lent, P. D. Tougaw, W. Porod and G. H. Bernstein, *Nanotechnology* **4**, 49 (1993).

[2] C. S. Lent, P. D. Tougaw, and W. Porod, *Appl. Phys. Lett.* **62**, 714 (1993).

[3] Douglas Tougaw and C. S. Lent, *J. Appl. Phys*. **80**, 4722 (1996).

[4] C. S. Lent and P. D. Tougaw, *Proc. IEEE*, **85**, 541 (1997).

[5] A. I. Csurgay, W. Porod, C. S. Lent, *IEEE Trans. on CAS-I*, **47**, 1212 (2000).

[6] G. Mahler and V. A. Weberruβ, *Quantum Networks* (Springer, 2nd Edition, 1998).

[7] G. Tóth, C.S. Lent, *J. Appl. Phys,* accepted; http://xxx.lanl.gov/abs/cond-mat/0104406.